

Changes in Cerebral Metabolism Are Detected Prior to Perfusion Changes in Early HIV-CMC: A Coregistered ^1H MRS and SPECT Study

Thomas Ernst, PhD,^{1,2*} Emmanuel Itti, MD,² Laurent Itti, PhD,² and Linda Chang, MD²

Human immunodeficiency virus-cognitive motor complex (HIV-CMC), a common complication of the acquired immunodeficiency syndrome (AIDS), is characterized by progressive cognitive impairment and motor dysfunction. Functional imaging methods, such as single-photon emission computed tomography (SPECT) and proton magnetic resonance spectroscopy (^1H -MRS), have been applied to assess the severity of brain injury. However, it is unclear which of these two methods is more sensitive in detecting brain abnormalities in patients with early HIV-CMC. Twenty-four HIV-CMC patients were compared with 34 healthy subjects; each had quantitative SPECT (^{133}Xe -calibrated $^{99\text{m}}\text{Tc}$ -HMPAO) and quantitative ^1H -MRS. Both modalities were co-registered in order to assess regional cerebral blood flow (rCBF) and metabolite concentrations within the same voxel of interest in four brain regions (midfrontal and midparietal gray matter, temporoparietal white matter, and basal ganglia). On SPECT, only the temporoparietal white matter showed a trend for decreased rCBF in HIV-CMC patients (-13% , $P = 0.06$). On MRS, HIV-CMC patients showed significantly reduced creatine concentration in the basal ganglia (-8% , $P = 0.008$), as well as increased myoinositol concentrations in the basal ganglia ($+25\%$, $P = 0.01$) and the temporoparietal white matter ($+18\%$, $P = 0.08$). There was no significant correlation between SPECT and MRS variables in the patients in any region. ^1H MRS showed abnormal neurochemistry in the basal ganglia, whereas rCBF on SPECT was normal in the same region. This finding suggests that metabolite concentrations on ^1H MRS are better surrogate markers than rCBF measurements with SPECT for the evaluation of brain injury in early HIV-CMC. *J. Magn. Reson. Imaging* 2000;12:859–865. © 2000 Wiley-Liss, Inc.

Index terms: HIV; brain; dementia; SPECT; magnetic resonance spectroscopy

THE SYNDROME of human immunodeficiency virus-cognitive motor complex (HIV-CMC) (1,2) occurs in 10%–20% of patients with the acquired immunodeficiency syndrome (AIDS) (3). With highly active antiretroviral therapy (HAART), the incidence of HIV-CMC is reduced by approximately 30% (4); however, it is unknown whether this reduced rate will remain stable. Clinically, patients with HIV-CMC develop progressive cognitive impairment and motor dysfunction (5,6). These symptoms may be related to the indirect effects of virally induced cytokines or the direct effect of HIV-1 viral proteins, which are present in high concentration in the subcortical structures, such as the globus pallidus, caudate, and deep white matter (7–11).

Neuropathologic findings in HIV-CMC patients include cerebrospinal fluid (CSF) abnormalities (12,13) and, in later stages of the syndrome, cerebral atrophy (14) with evidence of neuronal loss in the frontal cortex (15,16), volume reduction in the basal ganglia (17), white matter lesions (18,19) and vascular changes (17,19). Morphologic imaging techniques, such as computed tomography (CT) or MRI, are able to quantify in vivo structural changes occurring in gray and white matter (20–22). These changes may correlate with dementia severity or neuropsychological performance (23) but are generally more prominent during the later stages of HIV-associated dementia (22).

A variety of functional neuroimaging abnormalities have been reported in HIV-CMC, even during the early stages of the syndrome. Cortical perfusion defects and metabolic changes have been described using single-photon emission computed tomography (SPECT) or positron emission tomography (PET), particularly in the frontal cortex, and to a lesser extent in the temporal and parietal cortices and the deep gray matter (24–26). Several reports have characterized these gray matter abnormalities as multifocal defects (27–29), but only one study described perfusion changes in the white matter (28). The majority of the SPECT studies used $^{99\text{m}}\text{Tc}$ -hexamethyl-propylene amine oxime ($^{99\text{m}}\text{Tc}$ -HMPAO) and measured relative regional cerebral blood flow (rCBF), using cerebellar uptake as a reference (24,30). Some SPECT studies found abnormalities even in the early stages of the disease, before structural changes could be seen on MRI (31) or before cognitive

¹Department of Radiology, Harbor-UCLA Medical Center, Torrance, California 90502.

²Department of Neurology, Harbor-UCLA Medical Center, Torrance, California 90502.

Contract grant sponsor: NIDA, Scientist Development Award for Clinicians; Contract grant number: DA00280; Contract grant sponsor: GCRC; Contract grant number: MO1 RR00425.

*Address reprint requests to: T.E., Medical Department, Brookhaven National Laboratory, P.O. Box 5000, Upton, NY 11973. E-mail: ternst@bnl.gov

Received February 17, 2000; Accepted July 6, 2000.

impairments (32). PET showed decreased glucose metabolism in the white and gray matter, but hypermetabolism in the basal ganglia, during the early stage of HIV-CMC (33–35). More recently, perfusion MRI has also been shown to detect cerebral perfusion abnormalities in early HIV dementia (36,37).

Proton MR spectroscopy ($^1\text{H-MRS}$) is another functional neuroimaging technique that shows promise in the evaluation of brain injury in HIV-CMC. Studies in HIV-infected patients showed decreased ratio of N-acetyl aspartate/creatine (NA/CR) (38–40), increased choline/creatine (CHO/CR) (39,41), and increased myoinositol/creatine (MI/CR) (42,43). Using absolute concentration measurements, we confirmed that these changes in metabolite ratios were due to increased myoinositol concentration [MI] and, to a lesser extent, increased [CR] and [CHO], which correlated with the severity of HIV-CMC (44,45).

The main goal of this study was to compare the sensitivity of quantitative SPECT (assessing rCBF) and quantitative $^1\text{H-MRS}$ (assessing neurochemistry) for detecting consistent brain abnormalities in a group of patients with early stages of HIV-CMC. A secondary goal was to determine whether rCBF abnormalities correlate with abnormalities in brain metabolite concentrations.

MATERIALS AND METHODS

Subjects

Twenty-four HIV-positive subjects (21 men and three women), aged 26–63 years (39.5 ± 8.5 years), were compared with 37 healthy control subjects (34 men and three women), aged 24–63 years (38.3 ± 9.2 years). The subjects were recruited from the local community; each signed an informed consent form approved by the Human Subjects Institutional Review Board at Harbor-UCLA Research and Education Institute. All HIV patients underwent a detailed medical history and physical examination, a battery of screening blood tests (including complete blood count, routine chemistry, CD4 count, thyroid function tests, and syphilis serology), a drug use history (nine males had a history of cocaine dependence), and a neurologic evaluation and neuropsychological tests to determine AIDS dementia stage according to the Memorial Sloan-Kettering system (46). All HIV patients were in the early stages of HIV-CMC, with a mean AIDS dementia complex (ADC) stage of 0.48 ± 0.34 . Healthy control subjects were excluded if they had any chronic medical illnesses or a history of illicit drug or alcohol abuse. In each subject, MRI, $^1\text{H-MRS}$, and SPECT were acquired on the same day.

MRI and $^1\text{H-MRS}$

MRI and MRS were performed on a 1.5-T scanner (Signa, General Electric Medical Systems, Milwaukee, WI). Each examination included a sagittal T1-weighted spin-echo scan [(TE/TR 11/500 msec, 4-mm slice thickness, 1-mm gap, 24-cm field of view (FOV)], followed by either a fast axial T2-weighted multiecho scan (TE1/TE2/TR 17/102/4000 msec, 24-cm FOV, 5-mm

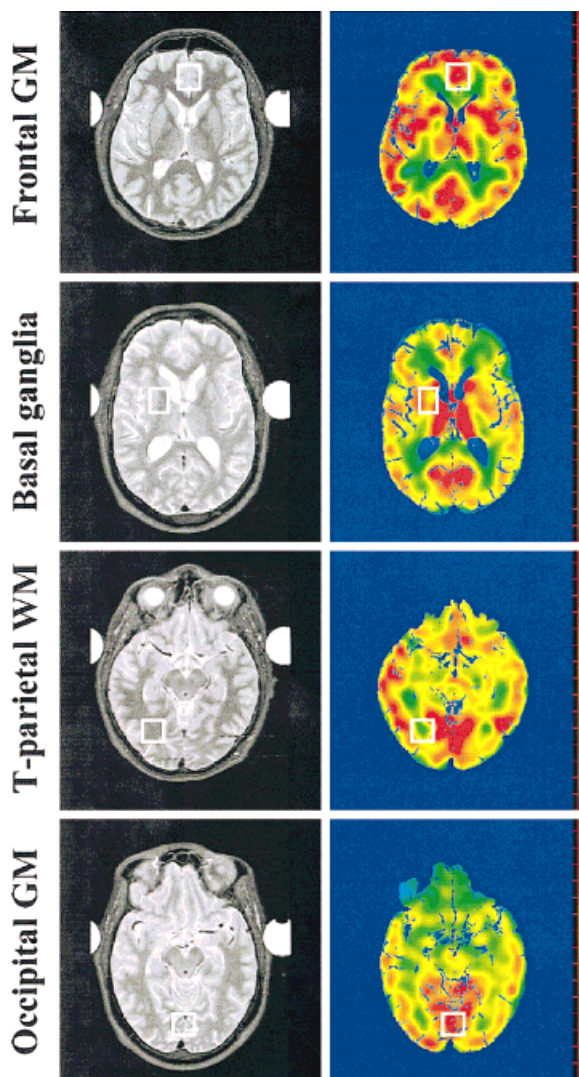


Figure 1. Four slices of an MRI scan and co-registered SPECT (atrophy corrected) from a control subject and a patient with HIV-CMC (ADC stage = 0.5, CD4 = 5/mm³). The four voxel locations are indicated on both modalities.

slice thickness, no gap) or a fast axial inversion recovery scan (TE/TI/TR 32/120/4000 msec, 24-cm FOV, 3.5-mm slice thickness, no gap).

Localized $^1\text{H-MRS}$ was performed using a STEAM sequence (47) (TE/TM/TR 30/13.7/2000 msec, 128 excitations) in the right temporoparietal white matter (8 patients, 13 controls) and the midoccipito-parietal gray matter (9 patients, 12 controls). In a separate set of subjects, ^1H spectra were acquired with an optimized PRESS sequence (48,49) (TE/TR 30/3000 msec, 128 averages, 2048 data points, 2.5 kHz bandwidth) in the midfrontal gray matter (15 patients, 13 controls) and in the right basal ganglia (14 patients, 12 controls). Voxel sizes ranged between 3 and 8 ml depending on the individual anatomy of the subject (Fig. 1). To avoid the ambiguities caused by the use of metabolite ratios, metabolite concentrations were determined using a method described previously (50,51). Briefly, the T2 decay of the water signal from the voxel was measured at 10 different echo times, separating the partial vol-

umes of CSF and brain tissue within the voxel. The brain tissue water signal was used as a reference, yielding metabolite concentrations in mmoles/kg corrected for CSF content. For comparison of our data with those from previous studies, we also determined metabolite ratios using creatine as an internal standard.

Data processing included the following steps: low frequency filtering of the FID (52), apodization (0.5 Hz Gauss broadening), zero filling, Fourier transformation, and manual zero-order phase correction. Next, an automatic DC baseline correction was performed using the signal intensities at 0 and 2.75 ppm. The peak areas of NA, CR, CHO, and MI were determined by integration and by fitting a Lorentzian line to each peak, separately for each baseline correction scheme. The resulting four areas per peak were averaged and referenced to the signal amplitude of the brain tissue water (50,51). This approach yields interindividual variations of about 10% and intrasubject variabilities of 3%–8%, for the major metabolite peaks (49). The relaxation times (T1 and T2) of the metabolites were assumed to be identical for both patients and control subjects.

SPECT

All HIV patients and normal subjects were evaluated with both ¹³³Xe (Dupont, Billerica, MA) and ^{99m}Tc-HMPAO (Ceretek, Amersham, Arlington Heights, IL), using a brain-dedicated scanner with three detectors (Headtome II, Shimadzu). The ¹³³Xe clearance method (53) provided an absolute quantitation of rCBF for 3 axial slices (64 × 64 pixels matrices, spatial resolution 20 mm). For these scans, subjects inhaled an air-¹³³Xe mixture (1110 MBq/L) for 1 minute. A ^{99m}Tc-HMPAO SPECT scan rendered qualitative images of cerebral perfusion at higher spatial resolution (10 mm in-plane, 16 mm slice thickness). Radiotracer (1110 Mbq) was administered intravenously within a quiet and dimly lit room. One hour after injection, 12 partially overlapping slices were acquired. Finally, the ¹³³Xe images were used to calibrate the HMPAO data set on a global basis for absolute rCBF (54,55).

Image Processing

To co-register the HMPAO images with the high-resolution MRI scans, both data sets were transferred to a UNIX workstation. After extracting the external brain surfaces from both the HMPAO and MRI scans, the two surfaces were matched and the SPECT scan was resliced according to the axial MRI slices (56). The registration accuracy of this algorithm is approximately 2–3 mm (56). The fused images (Fig. 2) were further corrected for the partial volume effect due to CSF (and thus for any cerebral atrophy) after segmentation of the CSF from the anatomic MRI scans (57). The structural MRI and segmented CSF images were also used to determine the total brain and CSF volumes in each subject. Volumes of interest (VOIs) were defined at the exact location of the spectroscopy voxels, by entering the voxel coordinates and size used for MRS data acquisition. The absolute rCBF in each VOI was then determined by applying the VOI to the co-registered and calibrated HMPAO map.

Statistical analysis

Analyses were performed in Statview (Abacus, Berkeley, CA). For each voxel location and each spectroscopy technique (STEAM or PRESS), we first compared the rCBF value, the three spectroscopy ratios (NA/CR, CHO/CR, and MI/CR), and the four metabolite concentrations ([NA], [CR], [CHO], [MI]) between HIV patients and normal subjects using unpaired Student's *t*-test. Linear regression analyses, separately for each brain region, were performed to assess the relationship between rCBF and each of the cerebral metabolite concentrations. For variables that showed a significant correlation, stepwise linear regression analyses, based on inclusion of variables, were additionally performed to evaluate the effect of metabolite concentrations and age on rCBF. All results are reported as mean ± standard deviation; *P* values of ≤ 0.05 were considered significant.

RESULTS

Morphologic imaging (MRI) showed structural abnormalities in five HIV patients; four showed slight cortical atrophy with ventricular enlargement, and one showed a white matter lesion in the left superior frontal lobe (5 × 2 × 3 cm³, hyperintense on T2-weighted images), without gray matter involvement. MR images were considered radiologically normal in the remainder of the HIV patients and all healthy controls. The global CSF volume of the HIV patients (135.8 ± 61.7 mL) was slightly, but not significantly, larger compared with the control subjects (123.3 ± 40.2 mL). Likewise, global brain volumes were smaller, but not significantly different, in the HIV patients (1295 ± 166 mL) compared with the control subjects (1349 ± 133 mL).

On SPECT, HIV patients showed a trend for reduced rCBF compared with control subjects only in the temporoparietal white matter region (–13%, *P* = 0.06; Table 1). With our small sample size, no significant differences were observed between HIV patients who had used cocaine in the past and those who had not.

Table 1 also shows the ¹H-MRS findings in the HIV-patients and the control subjects. In the HIV patients, the [NA] was normal in all regions, whereas the [CR] was decreased in the right basal ganglia region (–8%; *P* = 0.008). In addition, HIV patients showed significantly increased [MI] in the right basal ganglia region (+25%; *P* = 0.01) and a trend for increased [MI] in the right temporal white matter (+18%; *P* = 0.08). These abnormalities were associated with increases in the corresponding MI/CR ratios. In contrast, the increased NA/CR ratio in the HIV patients was due to the decreased [CR] but normal [NA].

In the HIV patients, there was no significant relationship between the rCBF and any of the metabolite concentrations. In contrast, the normal subjects showed an inverse correlation between [MI] and rCBF in the midfrontal gray matter (*r* = –0.74, *P* = 0.004) and between the [CHO] and rCBF in the basal ganglia (*r* = –0.60, *P* = 0.04); age did not contribute significantly as a variable in the stepwise regression analyses in both models. Furthermore, the CHO/CR ratio (but not age)

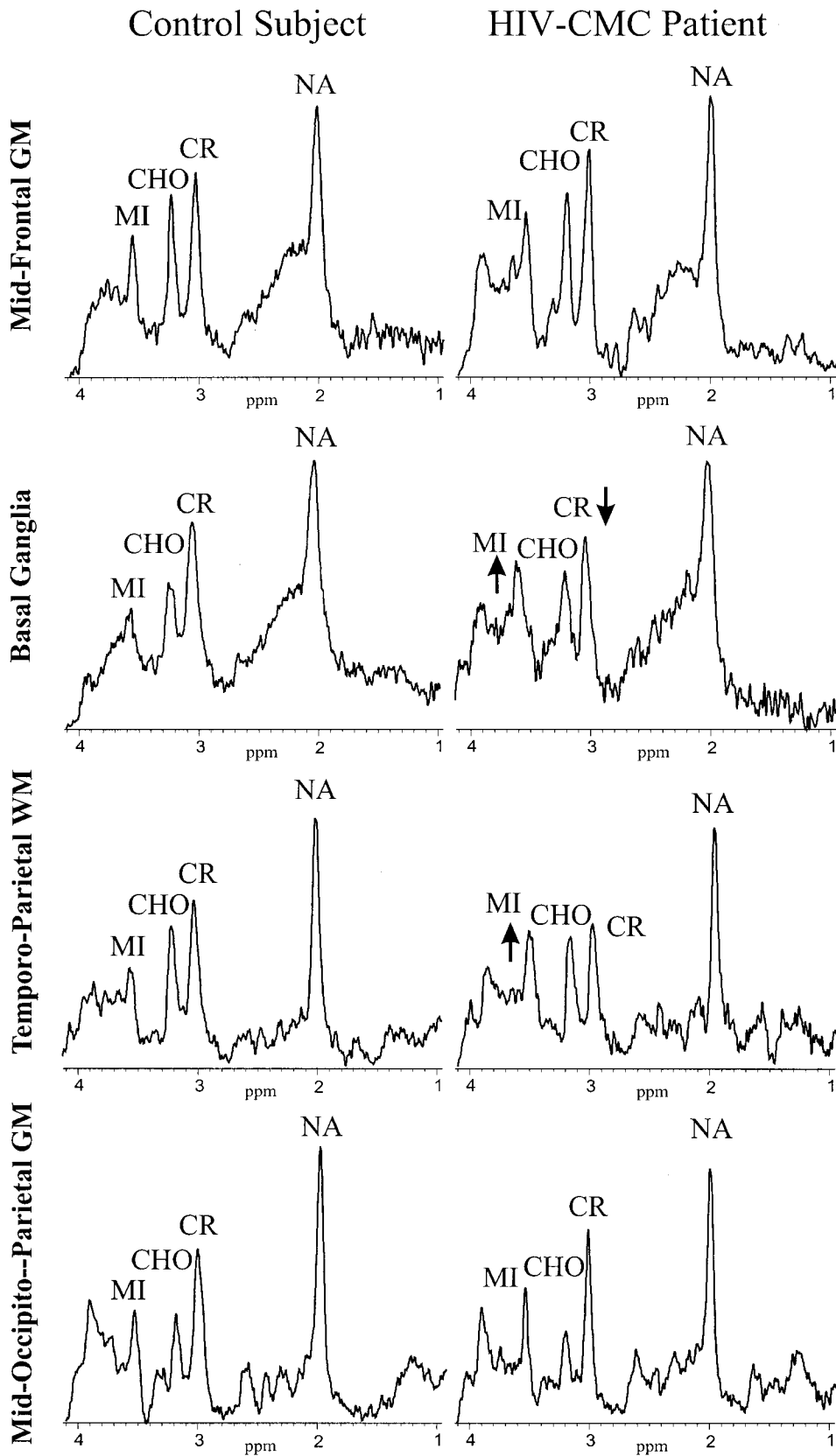


Figure 2. Representative ^1H -MR spectra from normal subjects and HIV-CMC patients, for each of the four voxel locations evaluated.

and rCBF in the temporoparietal white matter were correlated negatively ($r = -0.592$, $P = 0.03$). Since normal white matter generally has lower perfusion but higher [CHO] compared with gray matter (see Table 1),

these correlations might be due to variations in the white-to-gray matter ratio, especially in the basal ganglia region, which has a variable admixture of white and gray matter.

Table 1
Regional Cerebral Blood Flow (rCBF) and Brain Metabolite Ratios and Concentrations in Control and HIV-CMC Subjects

Voxel location	rCBF (mL/min/100 g)	NA/CR (%)	CHO/CR (%)	MI/CR (%)	[NA] (mmol/kg)	[CR] (mmol/kg)	[CHO] (mmol/kg)	[MI] (mmol/kg)
Mid-frontal gray matter								
Normal (<i>n</i> = 13)	59.33 ± 6.17	1.51 ± 0.15	0.84 ± 0.09	0.77 ± 0.05	8.54 ± 0.38	7.46 ± 0.74	2.13 ± 0.28	8.66 ± 1.38
HIV (<i>n</i> = 15)	56.92 ± 9.21	1.48 ± 0.11	0.83 ± 0.08	0.79 ± 0.09	8.56 ± 0.56	7.72 ± 0.55	2.16 ± 0.27	8.99 ± 1.26
<i>P</i> -values*	n.s.	n.s.	n.s.	n.s.	n.s.	n.s.	n.s.	n.s.
Right temporo-parietal white matter								
Normal (<i>n</i> = 13)	39.00 ± 6.55	1.49 ± 0.16	0.81 ± 0.11	0.56 ± 0.08	8.81 ± 1.01	6.33 ± 0.65	1.59 ± 0.28	6.68 ± 1.13
HIV (<i>n</i> = 8)	33.92 ± 4.77	1.39 ± 0.19	0.81 ± 0.12	0.70 ± 0.11	8.43 ± 1.08	6.09 ± 0.69	1.48 ± 0.26	7.91 ± 1.96
<i>P</i> -values*	<i>P</i> = 0.06	n.s.	n.s.	<i>P</i> = 0.004	n.s.	n.s.	n.s.	<i>P</i> = 0.08
Mid-occipito-parietal gray matter								
Normal (<i>n</i> = 13)	50.73 ± 9.63	1.39 ± 0.11	0.55 ± 0.07	0.55 ± 0.05	9.24 ± 1.03	8.04 ± 1.02	1.43 ± 0.30	7.26 ± 1.41
HIV (<i>n</i> = 9)	48.45 ± 9.00	1.33 ± 0.17	0.51 ± 0.08	0.56 ± 0.04	9.15 ± 0.97	8.51 ± 1.66	1.33 ± 0.26	7.68 ± 1.34
<i>P</i> -values*	n.s.	n.s.	n.s.	n.s.	n.s.	n.s.	n.s.	n.s.
Right basal ganglia								
Normal (<i>n</i> = 12)	56.25 ± 7.18	1.26 ± 0.12	0.77 ± 0.08	0.59 ± 0.10	8.97 ± 0.85	9.11 ± 0.74	2.28 ± 0.33	7.63 ± 1.13
HIV (<i>n</i> = 14)	55.06 ± 10.38	1.48 ± 0.11	0.83 ± 0.13	0.73 ± 0.15	9.10 ± 0.71	8.40 ± 0.51	2.36 ± 0.28	9.52 ± 2.14
<i>P</i> -values*	n.s.	<i>P</i> = 0.0001	n.s.	<i>P</i> = 0.01	n.s.	<i>P</i> = 0.008	n.s.	<i>P</i> = 0.01

All values are reported as mean ± standard deviation. **P*-values are from unpaired t-tests (two-tailed, n.s. = not significant). [NA] = N-acetyl concentration, [CR] = total creatine concentration, [CHO] = concentration of choline-containing compounds, [MI] = myoinositol concentration.

DISCUSSION

Cerebral Perfusion Changes on SPECT

In several functional neuroimaging studies of HIV patients, hypoperfusion has been observed even in the early course of the disease, despite relatively normal structural imaging (28,32,36,37,58,59). However, the majority of the SPECT studies described only a decrease in relative perfusion (32,59). Only one study measured absolute rCBF with ¹³³Xe-SPECT (58) and showed decreased rCBF in various brain regions in 16 of 18 HIV-positive patients. Some authors found increased perfusion and glucose metabolism in the basal ganglia of HIV patients (30,33,34,36). Using quantitative methods, the current study found only a trend for decreased rCBF in the temporoparietal white matter, with no change in rCBF in the cortical or subcortical gray matter. Our findings are consistent with neuropathologic studies, which show that abnormalities in early HIV-CMC occur preferentially in the white matter (8,19). To our knowledge, only one SPECT study evaluated blood flow in the white matter and found that, based on visual interpretation, AIDS patients showed multifocal subcortical defects (28).

The lack of abnormal (reduced) rCBF in the cortical regions of our study might be due to several factors. First, our patients had very early stages of HIV-CMC (ADC score < 1); perfusion abnormalities may be expected to be subtle in these patients. Second, our study evaluates for quantitative rCBF differences that consistently occur between HIV patients and control subjects. In contrast, many of the previous nuclear medicine studies assessed cerebral perfusion on an individual basis, often using visual interpretation. The perfusion abnormalities apparent in some of the patients, which were characterized as multifocal defects in various

brain regions, do not necessarily lead to consistent abnormalities in a patient group as a whole. Third, unlike previous studies, we corrected our SPECT data for brain atrophy, ie, the presence of excess CSF in each SPECT voxel. Without such a correction, increased atrophy in the brains of HIV patients may appear erroneously as decreased perfusion on the low-resolution SPECT scans, because there is no appreciable uptake of radiotracer in the CSF (volume dilution). Furthermore, measuring absolute blood flow on SPECT may result in increased variation compared with the relative rCBF measures often employed in SPECT studies; this may have decreased the statistical power to detect rCBF abnormalities. However, our data would have allowed us to detect changes as small as 5% in the absolute rCBF of the HIV patients. Finally, our analysis was limited to four brain regions in which the MRS was performed; therefore, it is possible that perfusion abnormalities were present in brain regions that were not included in our sample.

Cerebral Metabolite Changes on ¹H MRS

Many previous MRS studies have shown metabolite changes in the brain due to direct HIV infection, mostly using metabolite ratios. Characteristic findings in HIV patients are reduced NA/CR ratio, increased CHO/CR, and increased MI/CR. The results of this study demonstrate that the [MI] is elevated in the temporoparietal white matter and basal ganglia of the HIV patients, which is consistent with previous studies (42,43,45). Myoinositol is generally considered a glial marker (60). Therefore, increased [MI] in the white matter and basal ganglia suggests that these regions show glial activation early in the course of the disease; an interpretation that is consistent with post-mortem findings (8,17,19).

The findings of increased [MI] in the temporoparietal white matter (this study) and in the frontal white matter (45), as well as other metabolite abnormalities on spectroscopic imaging studies (61), indicate that HIV brain infection has a more pronounced effect in certain brain regions; however, the results probably are not highly dependent on the exact location of the voxels in the brain.

Many of the previous MRS studies found a decreased NA/CR ratio, which was generally interpreted as decreased NA. In this study, however, the [NA] is in the normal range in all four brain regions; this result is consistent with previous findings in patients with early HIV-CMC (45,61). Because the NA peak comprises primarily N-acetyl-aspartate, a neuronal marker (62), the normal [NA] indicates absence of substantial neuronal loss or damage in early HIV-CMC. The increased NA/CR in the basal ganglia of the HIV patients in this study is due only to a decreased [CR]; this finding exemplifies the inherent ambiguity associated with the interpretation of metabolite ratios.

The metabolite concentrations measured in the control subjects are in general agreement with those obtained in our previous studies (49,51). The use of short echo times (TE 30 msec) and long TR values (3 seconds) minimizes the effect of metabolite relaxation times on the measured metabolite concentrations. Similarly, using the brain water signal from within each MRS voxel as a concentration reference eliminates the influence of radiofrequency inhomogeneities on the concentration values. The application of two different localization techniques in this study most likely leads to some systematic errors that make it difficult to compare regional metabolite concentrations. However, such systematic errors probably had no influence on comparisons between patients and control subjects, since the corresponding data were always acquired with the same techniques.

Comparison of SPECT and ¹H-MRS in the Evaluation of HIV-CMC

In our study, both ¹H-MRS and SPECT showed a trend for abnormalities in the temporoparietal white matter of the HIV-CMC patients. In contrast, rCBF on SPECT was normal in the basal ganglia, one of the most severely affected brain regions in HIV-CMC, whereas ¹H MRS showed a marked increase of [MI] in this region. Consequently, ¹H MRS appears to have a higher sensitivity than SPECT for detecting brain injury in early HIV-CMC. Furthermore, metabolite concentrations on ¹H-MRS, but not rCBF on SPECT, have been shown to correlate well with clinical assessments of disease severity of HIV-CMC (45) and to reflect improvements in cerebral abnormalities after treatment with HAART (44). Therefore, given the existing data, metabolite abnormalities on ¹H MRS appear to be better "surrogate markers" for assessing the severity of brain injury in HIV-CMC than rCBF on SPECT.

ACKNOWLEDGMENTS

L.C. was the recipient of a Scientist Development Award for Clinicians (NIDA grant DA00280). We thank the

technical staff from the Harbor-UCLA Imaging Center and Oliver Speck, PhD, for his help with data analysis.

REFERENCES

1. Navia BA, Jordan BD, Price RW. The AIDS dementia complex: I. Clinical features. *Ann Neurol* 1986;19:517-524.
2. American Academy of Neurology AIDS Task Force Working Group. Report of a Working Group of the American Academy of Neurology AIDS Task Force. Nomenclature and research case definitions for neurologic manifestations of human immunodeficiency virus-type-1. *Neurology* 1991;41:778-785.
3. Qureshi A, Hanson D, Jones J, Janssen R. Estimation of the temporal probability of the human immunodeficiency virus (HIV) dementia after risk stratification for HIV-infected persons. *Neurology* 1998;50:392-397.
4. Sacktor N, Lyles R, McFarlane G, et al. HIV-1 related neurological disease incidence changes in the era of highly active antiretroviral therapy. *Neurology* 1999;52:A252-A253.
5. Levy RM, Bredesen DE, Rosenblum ML. Neurological manifestations of the acquired immune deficiency syndrome (AIDS): experience at UCSF and review of the literature. *J Neurosurg* 1985;62:475-495.
6. Janssen RS, Saykin AJ, Cannon L, et al. Neurological and neuropsychological manifestations of HIV-1 infection: association with AIDS-related complex but not asymptomatic HIV-1 infection. *Ann Neurol* 1989;26:592-600.
7. Navia BA, Cho ES, Petito CK, Price RW. The AIDS dementia complex: II. Neuropathology. *Ann Neurol* 1986;19:525-535.
8. Budka H, Costanzi G, Cristina S, et al. Brain pathology induced by infection with the human immunodeficiency virus (HIV). A histological, immunocytochemical and electron microscopical study of 100 autopsy cases. *Acta Neuropathol* 1987;75:185-198.
9. Price RW, Brew B, Sidtis J, Rosenblum M, Scheck AC, Cleary P. The brain in AIDS: central nervous system HIV-1 infection and AIDS dementia complex. *Science* 1988;239:586-592.
10. Kure K, Weidenheim KM, Lyman WD, Dickson DW. Morphology and distribution of HIV-1 gp41-positive microglia in subacute AIDS encephalitis. *Acta Neuropathol (Berl)* 1990;80:393-400.
11. Pulliam L, Herndier BG, Tang NM, McGrath MS. Human immunodeficiency virus-infected macrophages produce soluble factors that cause histological and neurochemical alterations in cultured human brains. *J Clin Invest* 1991;87:503-512.
12. Levy JA, Shimabukuro J, Hollander H, Mills J, Kaminsky L. Isolation of AIDS-associated retrovirus from cerebrospinal fluid and brain of patients with neurological symptoms. *Lancet* 1985;2:586-588.
13. McArthur JC, McClernon DR, Cronin MF, et al. Relationship between human immunodeficiency virus-associated dementia and viral load in cerebrospinal fluid and brain. *Ann Neurol* 1997;42:689-698.
14. Subbiah P, Mouton P, Fedor H, McArthur JC, Glass JD. Stereological analysis of cerebral atrophy in human immunodeficiency virus-associated dementia. *J Neuropathol Exp Neurol* 1996;55:1032-1037.
15. Everall IP, Luthert PJ, Lantos PL. Neuronal loss in the frontal cortex in HIV infection. *Lancet* 1991;337:1119-1121.
16. Ketzler S, Weis S, Haug H, Budka H. Loss of neurons in the frontal cortex in AIDS brains. *Acta Neuropathol* 1990;41:778-785.
17. Gray F, Lesc MC, Keohane C, et al. Early brain changes in HIV infection: neuropathological study of 11 HIV seropositive, non-AIDS cases. *J Neuropathol Exp Neurol* 1992;51:177-185.
18. Gray F, Scaravilli F, Everall I, et al. Neuropathology of early HIV-1 infection. *Brain Pathol* 1996;6:1-15.
19. Power C, Kong PA, Crawford TO, et al. Cerebral white matter changes in acquired immunodeficiency syndrome dementia: alterations of the blood-brain barrier. *Ann Neurol* 1993;34:339-350.
20. Dal Pan GJ, McArthur JH, Aylward E, et al. Patterns of cerebral atrophy in HIV-1-infected individuals: results of a quantitative MRI analysis. *Neurology* 1992;42:2125-2130.
21. Aylward EH, Henderer JD, McArthur JC, et al. Reduced basal ganglia volume in HIV-1-associated dementia: results from quantitative neuroimaging. *Neurology* 1993;43:2099-2104.
22. Aylward EH, Brettschneider PD, McArthur JC, et al. Magnetic resonance imaging measurement of gray matter volume reductions in HIV dementia. *Am J Psychiatry* 1995;152:987-994.

23. Hestad K, McArthur JH, Dal Pan GJ, et al. Regional brain atrophy in HIV-1 infection: association with specific neuropsychological test performance. *Acta Neurol Scand* 1993;88:112-118.
24. Holman BL, Garada B, Johnson KA, et al. A comparison of brain perfusion SPECT in cocaine abuse and AIDS dementia complex. *J Nucl Med* 1992;33:1312-1315.
25. Schwartz RB, Komaroff AL, Garada BM, et al. SPECT imaging of the brain: comparison of findings in patients with chronic fatigue syndrome, AIDS dementia complex, and major unipolar depression. *AJR* 1994;162:943-951.
26. Rosci MA, Pignorini F, Bernabei A, et al. Methods for detecting early signs of AIDS dementia complex in asymptomatic subjects: a quantitative tomography study of 18 cases. *AIDS* 1996;6:1309-1316.
27. Pohl P, Vogl G, Fill H, et al. Single photon emission computed tomography in AIDS dementia complex. *J Nucl Med* 1988;29:1382-1386.
28. Masdeu JC, Yudd A, Van Heertum RL, et al. Single photon emission computed tomography in human immunodeficiency virus encephalopathy: a preliminary report. *J Nucl Med* 1991;32:1471-1475.
29. Harris GJ, Pearlson GD, McArthur JC, Zeger S, LaFrance ND. Altered cortical blood flow in HIV-seropositive individuals with and without dementia: a single photon emission computed tomography study. *AIDS* 1994;8:495-499.
30. Dunlop O, Rootwelt K, Bjorklund R, et al. Reduced global cerebral blood flow in non-demented HIV positive patients. *J Neuro-AIDS* 1996;1:71-78.
31. Tatsch K, Schielke E, Bauer WM, et al. Functional and morphological findings in early and advanced stages of HIV infection. A comparison of 99mTc-HMPAO SPECT with CT or MRI studies. *Nuklearmedizin* 1990;29:252-258.
32. Shielke E, Tatsch K, Pfister HW, et al. Reduced cerebral blood flow in early stages of human immunodeficiency virus infection. *Arch Neurol* 1990;47:1342-1345.
33. Rottenberg DA, Moeller JR, Strother SC, et al. The metabolic pathology of the AIDS dementia complex. *Ann Neurol* 1987;22:700-706.
34. Rottenberg DA, Sidtis JJ, Strother SC, et al. Abnormal cerebral glucose metabolism in HIV-1 seropositive subjects with and without dementia. *J Nucl Med* 1996;37:1133-1141.
35. Adams MA, Ferraro FR. Acquired immunodeficiency syndrome dementia complex. *J Clin Psychol* 1997;53:767-778.
36. Tracey I, Hamberg LM, Guimaraes AR, et al. Increased cerebral blood volume in HIV-positive patients detected by functional MRI. *Neurology* 1998;50:1821-1826.
37. Chang L, Ernst T, Leonido-Yee M, Speck O. Perfusion MRI detects rCBF abnormalities in early stages of HIV-cognitive motor complex. *Neurology* 2000;54:389-396.
38. Menon DK, Ainsworth JG, Cox IJ. Proton MR spectroscopy of the brain in AIDS dementia complex. *J Comput Assist Tomogr* 1992;16:538-542.
39. Chong WK, Sweeney B, Wilkinson ID, et al. Proton spectroscopy of the brain in HIV infection: correlation with clinical, immunologic and MR imaging findings. *Radiology* 1993;188:119-124.
40. McConnell JR, Swindells S, Ong CS, et al. Prospective utility of cerebral proton magnetic resonance spectroscopy in monitoring HIV infection and its associated neurological impairment. *Aids Research and Human Retroviruses* 1994;10:977-982.
41. Jarvik JG, Lenkinski RE, Grossman RI, et al. Proton MR spectroscopy of HIV-infected patients: characterization of abnormalities with imaging and clinical correlation. *Radiology* 1993;186:739-744.
42. Laubenberger J, Haussinger D, Bayer S, et al. HIV-related metabolic abnormalities in the brain: depiction with proton MR spectroscopy with short echo times. *Radiology* 1996;199:805-810.
43. Lopez-Villegas D, Lenkinski RE, Frank I. Biochemical changes in the frontal lobe of HIV-infected individuals detected by magnetic resonance spectroscopy. *Proc Natl Acad Sci USA* 1997;94:9854-9859.
44. Chang L, Ernst T, Leonido-Yee M, et al. Highly active antiretroviral therapy reverses brain metabolite abnormalities in mild HIV dementia. *Neurology* 1999;53:782-789.
45. Chang L, Ernst T, Leonido-Yee M, Walot I, Singer E. Cerebral metabolite abnormalities correlate with clinical severity of HIV-cognitive motor complex. *Neurology* 1999;52:100-108.
46. Aronow HA, Brew BJ, Price RW. The management of the neurological complications of HIV infection and AIDS. *AIDS* 1988;2:151-159.
47. Frahm J, Merboldt KD, Hänicke W. Localized proton spectroscopy using stimulated echoes. *J Magn Reson* 1987;72:502-508.
48. Bottomley PA. Spatial localization in NMR spectroscopy in vivo. *Ann NY Acad Sci* 1987;508:333-348.
49. Ernst T, Chang L. Elimination of artifacts in short echo time ¹H MR spectroscopy of the frontal lobe. *Magn Reson Med* 1996;36:462-468.
50. Ernst T, Kreis R, Ross BD. Absolute quantitation of water and metabolites in the human brain. I: Compartments and water. *J Magn Reson* 1993;B102:1-8.
51. Kreis R, Ernst T, Ross BD. Absolute quantitation of water and metabolites in the human brain. II: Metabolite concentrations. *J Magn Reson* 1993;B102:9-19.
52. Kreis R, Farrow N, Ross BD. Localized ¹H NMR spectroscopy in patients with chronic hepatic encephalopathy. Analysis of changes in cerebral glutamine, choline and inositols. *NMR Biomed* 1991;4:109-116.
53. Kanno I, Lassen NA. Two methods for calculating regional cerebral blood flow from emission computed tomography of inert gas concentration. *J Comput Assist Tomogr* 1979;3:71-76.
54. Payne JK, Trivedi MH, Devous MDS. Comparison of technetium-99m-HMPAO and xenon-133 measurements of regional cerebral blood flow by SPECT. *J Nucl Med* 1996;37:1735-1740.
55. Andersen AR, Friberg H, Lassen NA, Kristensen K, Neirinckx RD. Serial studies of cerebral blood flow using 99mTc-HmPAO: a comparison with ¹³³Xe. *Nucl Med Commun* 1987;8:549-557.
56. Itti L, Chang L, Mangin JF, Darcourt J, Ernst T. Robust multimodality registration for brain mapping. *Hum Brain Map* 1997;5:3-17.
57. Itti L, Chang L, Ernst T, Mishkin F. Improved 3-D correction for partial volume effects in brain SPECT. *Hum Brain Map* 1997;5:379-388.
58. Tran Dinh YR, Mamo H, Cervoni J, Caulin C, Saimot AC. Disturbances in the cerebral perfusion of human immune deficiency virus-1 seropositive asymptomatic subjects: a quantitative tomography study of 18 cases. *J Nucl Med* 1990;31:1601-1607.
59. Sacktor N, Van Heertum RL, Dooneief G, et al. A comparison of cerebral SPECT abnormalities in HIV-positive homosexual men with and without cognitive impairment. *Arch Neurol* 1995;52:1170-1173.
60. Brand A, Richter-Landsberg C, Leibfritz D. Multinuclear NMR studies on the energy metabolism of glial and neuronal cells. *Dev Neurosci* 1993;15:289-298.
61. Barker PB, Lee RR, McArthur JC. AIDS dementia complex: evaluation with proton MR spectroscopic imaging. *Radiology* 1995;195:58-64.
62. Urenjak J, Williams SR, Gadian DG, Noble M. Proton nuclear magnetic resonance spectroscopy unambiguously identifies different neural cell types. *J Neurosci* 1993;13:981-989.